Progress In Electromagnetics Research M, Vol. 90, 117–125, 2020

Design and Analysis of a Compact and Excellent Out of Band Rejection E-CRLH Inspired Bandpass Filter

Mahmoud A. Abdalla[1], Dilip K. Choudhary[2], and Raghvendra K. Chaudhary[2, *]

Abstract—This paper introduces the design and analysis of a compact bandpass with sharp attenuation. The filter topology employs three different cells of a bisected-Π/Π configuration of a negative refractive index metamaterial transmission line. The filter centre frequency is 3.65 GHz, and its 3 dB cutoff frequencies are 2.55 GHz and 4.6 GHz (57% fractional bandwidth). The filter attenuation increases to 20 dB in only 100 MHz (at 4.7 GHz). Moreover, the filter has only 0.2 dB insertion loss within the passband. The filter stopband is characterized with typical flat with 0.2 dB return loss within the stopband (4.7 GHz–5.75 GHz) and very close to 20 dB insertion loss. Moreover, the filter has two frequency independent designed transmission zeros within this stopband. Along with previous specifications, the filter size is only $0.22\lambda_g \times 0.20\lambda_g$ ($12 \times 11\,\text{mm}^2$) at centre frequency. The filter performance has been validated through circuit model, electromagnetic simulation, and experimental measurements.

1. INTRODUCTION

Microwave filters are playing a great role in the development of wireless communication services [1]. The continuous development in wireless services requires the employed bandpass filters to become small in size and featured with challenging filter specifications [2].

Specifically, the compactness of microwave bandpass filters is a critical issue since it matches the recent small size microwave transceiver systems. Therefore, many miniaturization techniques have been used to miniaturize bandpass filter size. These techniques include using stub loading [3], reactive lumped elements loading [4–6], asymmetric coupled lines [7, 8], and coil transformer loading [9, 10].

On the other hand, several wideband filters have been presented with different techniques. In all of these filters, sharp attenuations and good out of band stopband characteristics are always in high demand [11–19].

Since artificial planar metamaterials transmission lines have proven novel properties in electromagnetic components community research, they have also been used to introduce wideband and compact filters [20–29]. Therefore, ultra-compact filter design based on these lines has become a very competitive design approach.

Moreover, since the introduction of the modified version of these lines such as generalized negative refractive index metamaterial (NRI-MTM) transmission lines [30] (extended composite right left handed (E-CRLH) transmission line [31]), they have been a subject for many novel microwave components. Based on such novel artificial transmission lines and their different extracted equivalent circuits, many microwave filters has been presented [32–35]. In these designs, the compactness, multi-band, and transmission zeros were always the main topic.

Received 25 December 2019, Accepted 5 March 2020, Scheduled 10 March 2020

* Corresponding author: Mahmoud A. Abdalla (maaabdalla@ieee.org).

[1] Electronic Engineering Department, Military Technical College, Cairo, Egypt. [2] Department of Electronics Engineering, Indian Institute of Technology (Indian School of Mines), Dhanbad-826004, India.

In this paper, a wideband, compact, and high attenuation bandpass filter based on E-CRLH transmission lines is introduced. The filter is designed for covering the microwave frequencies of wireless services from 2.65 to GHz to 4.6 GHz. Two transmission zeros are achieved within a typical stopband, and they are deeply emphasized. The paper emphasizes the transmission zeros in terms of electric field study and parametric study.

2. II-DESIGN PROCEDURES

The design approach of the designed filter is based on designing a cascaded combination of Extended Composite right/left cells. The two cells are designed to have wide bandpass response for the first cell whereas the second cell demonstrates a bandstop properties within the stopband of the first cell. As a result, the final filter has good bandpass properties with wide stopband. Through the whole paper, the proposed filters are designed using a Rogers 6010 substrate with a relative dielectric constant of 10.2, loss tangent of 0.0023, and thickness of 1.27 mm, and with a 50 Ω microstrip feed line.

The design of the wide passband E-CRLH cell is based on designing the cell with a PI configuration. Such a configuration is simple in having balanced condition with a wide impedance balance within the passband response. The dimensions of the cell are obtained after satisfying a cutoff at 3.5 GHz and 5 GHz. These conditions are satisfied by satisfying zero propagation phase constant (β) using the periodic dispersion relation in terms of the impedance Z and admittance Y (shown in Fig. 1(a)) as

$$\cos(\beta d) = 1 + ZY \tag{1}$$

$$Z = \frac{Z_{s1}Z_{s2}}{Z_{s1}+Z_{s2}}, \quad Z_{s1} = j\omega L_{R1} + \frac{1}{j\omega C_{L1}}, \quad Z_{s2} = j\omega L_{p1} \tag{2}$$

$$Y = Y_{p1} + Y_{p2} = (1/j\omega L_{L1}) + \left(j\omega C_{R1} + \frac{j\omega C_s}{1-\omega^2 L_s C_s}\right) \tag{3}$$

The filter design specifications are ($f_{c1} = 2.7$ GHz and $f_{c2} = 4.6$ GHz), corresponding to $\beta d \simeq 0$, and designing a pole at 3.7 GHz, corresponding to $\beta d \simeq \pi/2$. Assuming the parasitic effect ($L_{R1} = 0.4$ nH, $C_{R1} = 0.1$ pF), the designed values are $L_{L1} = 7.08$ nH, $C_{L1} = 0.59$ pF, $L_{p1} = 0.94$ nH, $C_s = 0.05$ pF, $L_s = 22.96$ nH.

Next, the loading elements are synthesized as shown in Fig. 1(b) as C_{L1} is an interdigital capacitor and C_s a patch capacitor. On the other hand, L_S and L_{L1} are thin strip segment inductances with different widths. Finally, L_{R1} and C_{R1} are patristic elements of the hosting microstrip transmission line, and they are obtained based on the size of the hosting microstrip transmission line and tuned based on circuit simulations. Comparing the equivalent circuit in Fig. 1(a) to the layout in Fig. 1(b), there is an axis of symmetry around which the two shunt configurations exist.

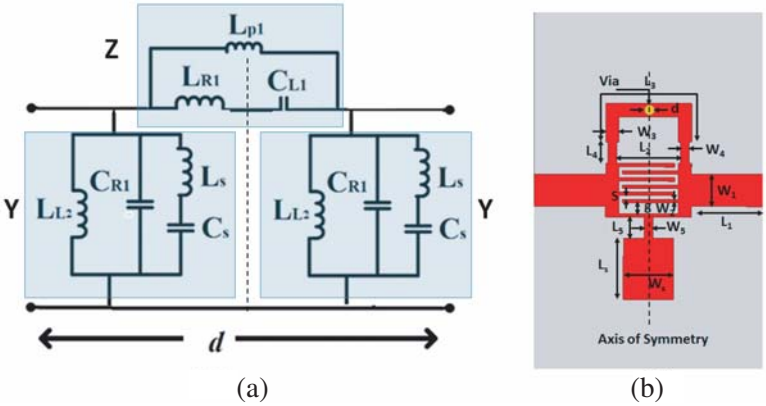

Figure 1. The wide band Π- E-CRLH cell, (a) equivalent circuit (a) filter layout $L_1 = 4.0$, $L_2 = 3.3$, $L_3 = 7.375$, $L_4 = L_5 = 1.2$, $L_s = 3.4$, $W_1 = 1.8$, $W_2 = 0.2$, $W_3 = 0.625$, $W_4 = W_5 = 0.5$, $W_s = 2.8$, $d = 0.2$, $s = 0.2$, $g = 0.8$].

It is worth to comment that the change of W_3 and W_4 in the strips is associated with the needed inductance value (L_{L2}) and at the same time to meet the available fabrication facilities.

By employing the commercial software (Ansoft-Design), the full wave simulated transmission coefficient (S_{21}) of the Π-CRLH cell is shown in Fig. 2. It is obvious that the cell has a passband response in the frequency band 3.5 GHz to 5.5 GHz, approximately. Above 5.5 GHz, the transmission coefficient starts to drop with bad attenuation rate which reaches only −4 dB at 6 GHz. On the other hand, in the frequencies below 3.5 GHz, the Π-E-CRLH cell has an imperfect roll off response such that it achieves −10 dB attenuation at 2 GHz. From previous results, it can be claimed that the designed cell cannot function perfect for the desired filter response. This point will be solved in the next attempt by adapting and cascading it with asymmetric half Π-E-CRLH cell.

The equivalent circuit of the half Π-E-CRLH cell is shown in Fig. 3(a) whereas the synthesized cell is shown in Fig. 3(b). Compared to the circuit in Fig. 1(a), it is obvious that the cell is one asymmetric half Π configuration. In contrast to the previous configuration in Fig. 1(a), the half Π configuration in Fig. 3(a) has a non-balanced impedance configuration which makes the passband narrower and stopband sharper. The elements are designed in the same way as the precious Π-E-CRLH cell to demonstrate cutoff frequencies at 3.5 GHz and 5 GHz.

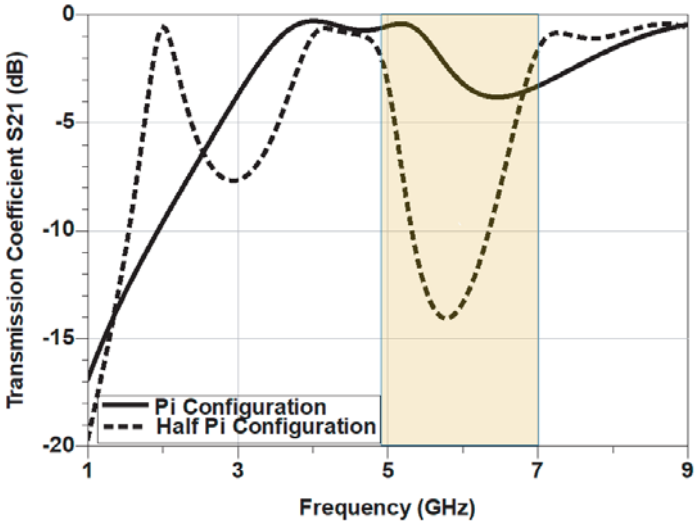

Figure 2. The simulated transmission coefficient (S_{21}) of the Π-E-CRLH cell versus the half Π-E-CRLH cell.

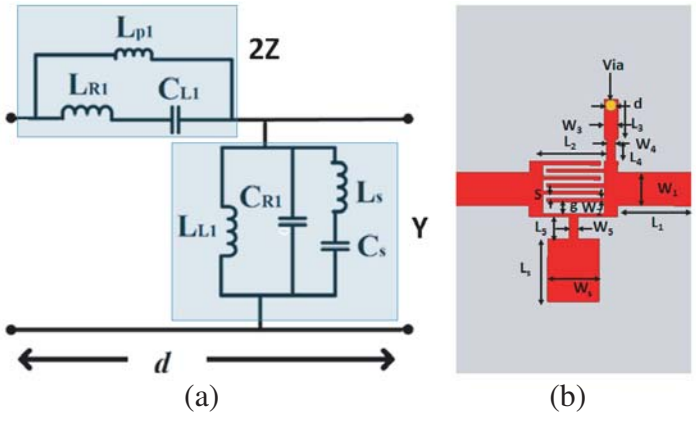

Figure 3. The wide band half Π-E-CRLH cell, (a) equivalent circuit (a) filter layout $L_1 = 4.0$, $L_2 = 3.3$, $L_3 = 2.375$, $L_4 = L_5 = 1.2$, $L_s = 3.4$, $W_1 = 1.8$, $W_2 = 0.2$, $W_3 = 0.625$, $W_4 = W_5 = 0.5$, $W_s = 2.8$, $d = 0.2$, $s = 0.2$, $g = 0.8$].

The simulated transmission coefficient (S_{21}) is shown in Fig. 2 where it is obvious that the cell can demonstrate the same passband frequencies but with sharper roll off attenuation. The transmission coefficient drops from −3 dB at 5 GHz to −15 dB at 5.9 GHz. On the other hand, at low roll off frequencies, it reaches −8 dB at 3.5 GHz. By comparing the results in Fig. 2, it can be claimed that by cascading the two cells, the passband filter with wide stopband characteristics can be achieved.

3. III-EXTENDED CRLH METAMATERIAL BANDPASS FILTER

The proposed equivalent circuit of the proposed filter is shown in Fig. 4. The filter is designed to cascade the Π-ECRLH cell with two half Π-ECRLH cells at ends. Thanks to this configuration, the band-pass properties of the filter is kept unchanged as that of the Π-ECRLH cell whereas the bandstop characteristics of the half Π-ECRLH cells help to create sharp wide stopband. Although the previously designed filters in Section 2 were the starting points, it is worth to comment that some fine tuning has been applied to the cascaded filter structure for achieving better results.

Finally, a detailed filter layout is shown in Fig. 5(a) whereas its fabricated prototype is shown in Fig. 5(b), and the filter topology is shown in Fig. 5(b). It is noted that the Π-CRLH cells share inductive arms in the realization step as shown in Fig. 5(a). The purpose of this is to achieve compactness. From circuit point of view in Fig. 4, L_{L1} and L_{L2} are parallel inductors, so they are realized as one inductor (L_L) whereas they are modeled as two inductors in the design stage.

Also, it is noted that there is a small shift in the rectangular stub in the three cells from the middle (axis of symmetry). The purpose of the shift of the rectangular stubs is to fine tune the cascaded filter matching. However, it is worth to claim that this shift effect on the equivalent circuit in Fig. 4 is not

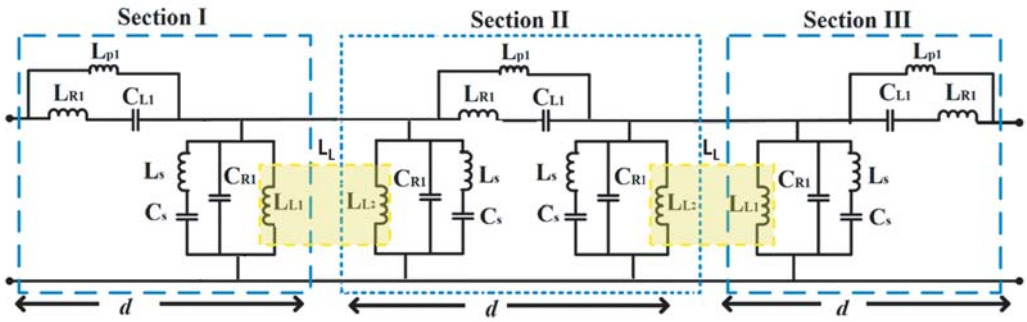

Figure 4. The equivalent circuit model of cascaded wide stop band E-CRLH BPF filter.

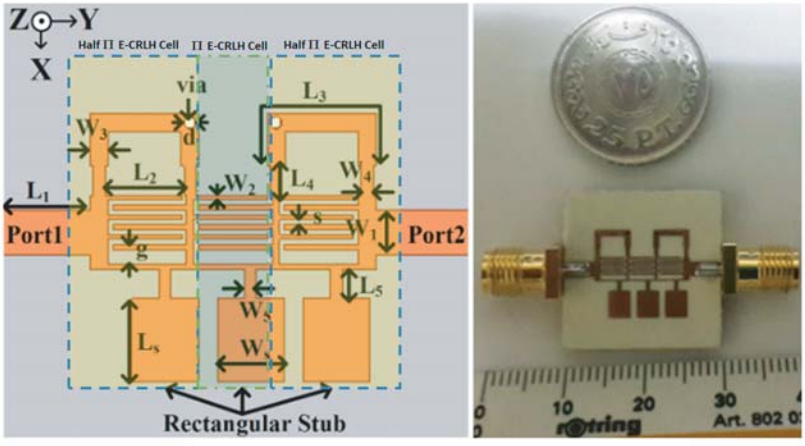

Figure 5. (a) The E-CRLH bandpass filter layout. (b) Fabricated prototype.

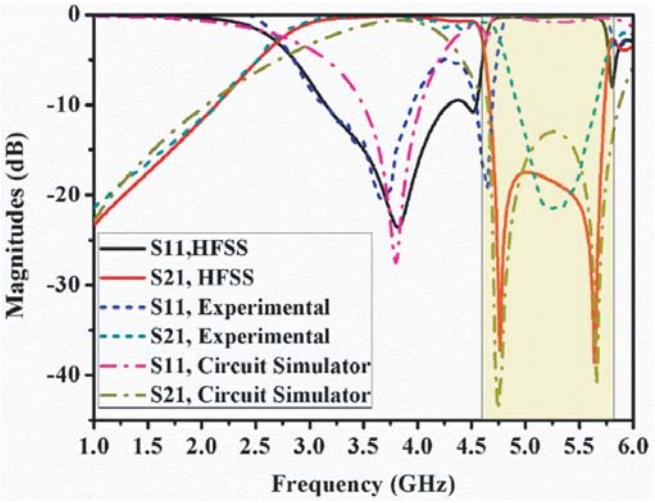

Figure 6. The Simulated and measured scattering parameters magnitudes of the proposed E-CRLH Filter.

significant.

For good evaluation of the achieved filter concept, the designed filter has been examined using both of circuit simulations and 3D EM simulations. The simulated results are shown in Fig. 6 where it is obvious that the filter has a bandpass filter response followed by bandstop properties. It is obvious that the circuit and full wave HFSS simulations are always identical whereas the measurement results are shifted about 100 MHz in passband cutoff frequencies.

Within the bandpass filter passband, it is clear that the filter achieves the cutoff frequencies (at which $S_{21} = 0.707 = -3\,\text{dB}$) at 2.7 GHz and 4.6 GHz. The filter has two poles frequencies (at which $S_{11} = 0$ at 3.8 GHz and 4.5 GHz). On the other hand, within the stopband the simulated filter results have two transmission zeros (at which $S_{21} = 0$) *at* 4.75 GHz and 5.65 GHz. In the measurement results, the two transmission zeros (TZs) are merged to one TZ at 5.25 GHz which can be claimed due to the non-avoided imperfection in fabrication process. The insertion loss is close to 0 ± 0.5 dB over the passband. Following this passband characteristic, the filter has a sharp stopband that ranges from 4.5 GHz to 5.8 GHz. Within this stopband, the return loss is almost 0 ± 0.5 dB; the attenuation is more than 20 dB over the whole band, and specifically it reaches 40 dB at 4.75 GHz and 5.65 GHz within the stopband.

It is worth to comment that the achieved results with proposed filter focus only on having high attenuation at upper side of the filter since in most signals interference, high frequency spectrum is more sensitive. Improvement of lower band is possible with other added techniques such as cascading the proposed filter with band notch filter whose attenuation band shares the same attenuation of lower side band.

4. TRANSMISSION ZEROS ANALYSIS DESIGN AND DISCUSSION

To analyze the response of the proposed filter, we introduce, in this section, the transmission zeros/poles of the filter which are analyzed and confirmed by the current distribution study.

First, in Fig. 7, the surface current densities of proposed filter at transmission zero frequencies are plotted. Fig. 7(a) reveals that maximum surface current density is found at the series resonator (the two studs L_{p1} and L_{R1} in parallel with the interdigital capacitor (IDC) C_{L1}). Hence, it can be claimed that this resonance can be controlled to be responsible for the first transmission zero at 4.75 GHz. Also, there is small effect on this transmission zeros which is controlled by the parallel resonator in shunt branch formed by the shorted stub (L_L) and the parasitic capacitance (C_R). On the other hand, Fig. 7(b) demonstrates the second transmission zero at 5.65 GHz. It can be noticed that the maximum surface current density is created within the series resonator (L_s and C_s) within the shunt branch, i.e.,

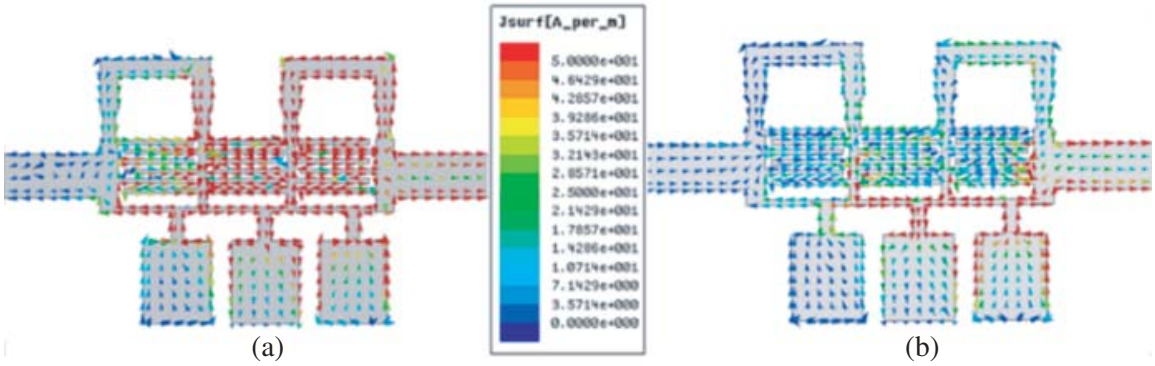

Figure 7. Surface current density at transmission zero frequencies, (a) At 4.75 GHz of bandpass filter, (b) At 5.65 GHz of bandpass filter.

at rectangular stub.

It is worth to comment that the former resonators not only control the transmission zeros but also control the main centre frequency (pole frequency). So, during the design a careful optimization process is conducted to achieve the goals.

To confirm the outcomes in Fig. 7, different parametric studies are performed. The position of transmission zeros can be independently controlled by varying the gap between fingers and width of IDC fingers as shown in Figs. 8 and 9, respectively. As space between interdigital fingers (s) increases, the value of the IDC changes. It is clear in Figure 8 that the first transmission zero position (TZ1) increases, and second transmission zero remains constant. This result confirms the current distribution at the series tank circuit in Fig. 8. However, it is obvious that the effect of centre filter frequency is unaffected by changing the gap (s). Controlling the centre frequency and TZ1 at the same time can be done making use of the patristic inductance of the IDC (L_R). Fig. 9 shows the variation in resonance frequency ($f_{01} = 3.8$ GHz) with respect to width of interdigital fingers (W_2). As W_2 increases, the interdigital capacitance decreases, and the resonance frequency (f_{01}) shifts towards higher value. Also, TZ1 is shifted up in the same manner.

From the current distribution in Fig. 7(b), it has become clear that the TZ2 is due to the resonance of the shunt tank circuit formed by L_C and C_S. Therefore, in Fig. 10, the effect of changing the rectangular stub L_s in terms of the capacitance C_s change is studied. It is obvious that when the length increases (capacitance C_s increases), the TZ1 remains constant, and TZ2 shifts towards lower value.

From the above analysis in Fig. 8, Fig. 9, and Fig. 10, it is quite clear that the proposed filer has the advantages of independently varying the transmission zeros positions with respect to series and shunt tank circuits.

Finally, a performance comparison of the proposed filter with recent filter is summarized in Table 1, where it can clearly confirm the power of the filter.

Table 1. A comparison between the proposed filter characteristics and other recent similar works.

Ref.	RF (GHz)	IL (dB)	RL (dB)	FBW (%)	TZ	Size ($\lambda_g \times \lambda_g$)
[11]	2.45	2.3	> 15	3.5	-	0.26×0.30
[12]	3.95	0.85	21	44	58	0.48×0.32
[13]	2.28	1.58	> 14	-	44	0.26×0.36
[14]	3.5	0.7	20	70	100	0.25×0.45
[15]	3.25	1.0	17	21.2	62	0.22×0.29
[32]	2.39	1.94	19.6	6.6	84	0.61×0.12
This work	3.65	0.6	22	56	85	0.20×0.22

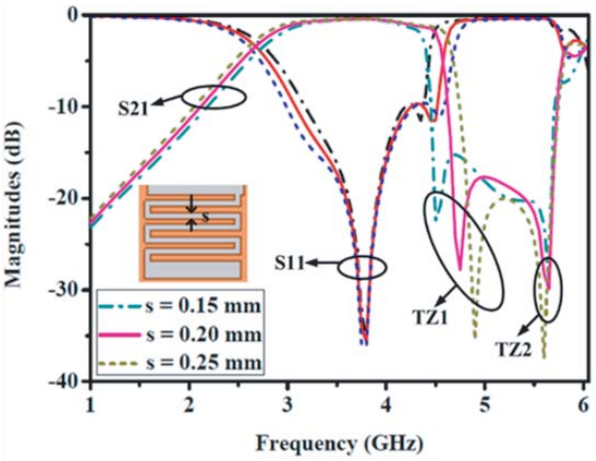

Figure 8. Scattering parameters magnitudes variation (Transmission zero variation) with respect to: Gap between IDC fingers (s).

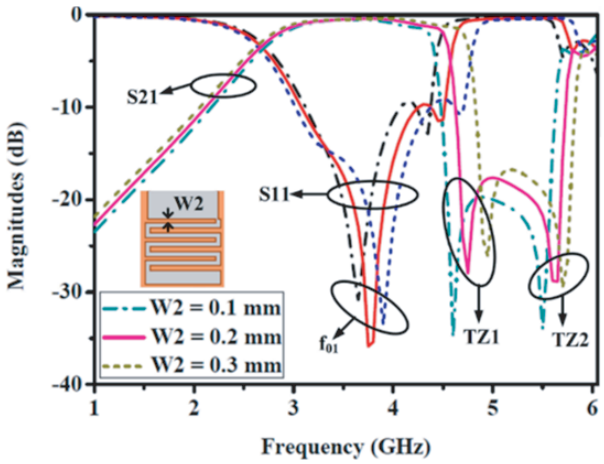

Figure 9. Scattering parameters magnitudes variation (Transmission zero variation) with respect to: Width of IDC (W2).

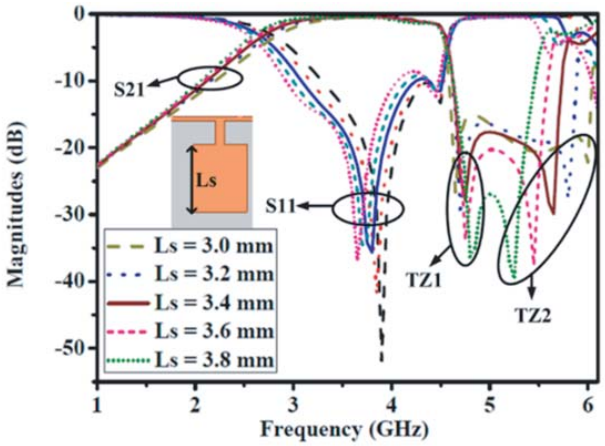

Figure 10. Scattering parameters magnitudes variation (Transmission zero variation) with respect to (c) Length of rectangular stub (Ls).

5. CONCLUSION

In this paper, design and analysis of a compact bandpass filter based on E-CRLH cells with two independent transmission zeros and wide stopband for Wi-Max frequencies (2.55 GHz–4.6 GHz) are introduced. With only three cascaded cells, two transmission zeros and one pole frequency have been achieved. Results are discussed based on circuit simulation, full wave EM simulation, and experimental measurements. The filter size is very competitive $0.22\lambda_g \times 0.2\lambda_g$ at centre frequency 3.65 GHz. Also, the filter has very sharp attenuation slope and good out of band rejection band (dropping from 3 dB to 20 dB in only 100 MHz).

REFERENCES

1. Hong, J. S., *Microstrip Filters for RF/Microwave Applications*, Wiley, New York, NY, USA, 2011.
2. Feng, W., W. Che, and Q. Xue, "Transversal signal interaction: Overview of high-performance wideband bandpass filters," *IEEE Microwave Magazine*, Vol. 15, No. 2, 84–96, 2014.

3. Zhang, Z.-C., S.-W. Wong, J.-Y. Lin, H. W. Liu, L. Zhu, and Y. J. He, "Design of multistate diplexers on uniform-and stepped-impedance stub-loaded resonators," *IEEE Transactions on Microwave Theory and Techniques*, Vol. 67, No. 4, 1452–1460, 2019.
4. Orellana, M., J. Selga, P. Vélez, M. Sans, A. Rodríguez, J. Bonache, V. E. Boria, and F. Martín, "Design of capacitively loaded coupled-line bandpass filters with compact size and spurious suppression," *IEEE Transactions on Microwave Theory and Techniques*, Vol. 65, No. 4, 1235–1248, 2017.
5. Lim, T., B.-W. Min, and Y. Lee, "Miniaturisation method for coupled-line bandpass filters with identical and minimal number of reactive elements," *IET Microwaves, Antennas & Propagation*, Vol. 8, No. 14, 1192–1197, 2014.
6. Lin, T.-W., J.-T. Kuo, and S.-J. Chung, "Dual-mode ring resonator bandpass filter with asymmetric inductive coupling and its miniaturization," *IEEE Transactions on Microwave Theory and Techniques*, Vol. 60, No. 9, 2808–2814, 2012.
7. Mo, Y. X., K. J. Song, and Y. Fan, "Miniaturized triple-band bandpass filter using coupled lines and grounded stepped impedance resonators," *IEEE Microwave and Wireless Components Letters*, Vol. 24, No. 5, 333–335, 2014.
8. Park, J.-H., S. Lee, and Y. Lee, "Extremely miniaturized bandpass filters based on asymmetric coupled lines with equal reactance," *IEEE Transactions on Microwave Theory and Techniques*, Vol. 60, No. 2, 261–269, 2011.
9. Huang, C.-C., W.-T. Fang, and Y.-S. Lin, "Miniaturization of broadband stub bandpass filters using bridged-T coils," *IEEE Access*, Vol. 6, 20164–20173, 2018.
10. Li, Y., C. Wang, and N.-Y. Kim, "Design of very compact bandpass filters based on differential transformers," *IEEE Microwave and Wireless Components Letters*, Vol. 25, 439–441, 2015.
11. Tang, M., T. Shi, and X. Tan, "A novel triple-mode hexagon bandpass filter with meander line and central-loaded stub," *Microwave and Optical Technology Letters*, Vol. 58, 9–12, 2015.
12. Tanni, K. and K. Wada, "Wideband bandpass filter composed of dual-path resonators using coupled-line and transmission line with inductive elements," *IEEE Microw. Wireless Compon. Lett.*, Vol. 24, 14–16, 2014.
13. Xiao, J. K., M. Zhu, Y. Li, and J. G. Ma, "Coplanar waveguide bandpass filters with separate electric and magnetic couplings," *Electronics Letter*, Vol. 52, 122–124, 2016.
14. Yechou, L., A. Tribak, M. Kacim, J. Zbitou, and A. M. Sanchez, "A novel wideband bandpass filter using coupled lines and T-shaped transmission lines with wide stopband on low-cost substrate," *Progress In Electromagnetics Research C*, Vol. 67, 143–152, 2016.
15. Wu, Y. D., G. H. Li, W. Yang, and X. Yang, "Design of compact wideband QMSIW band-pass filter with improved stopband," *Progress In Electromagnetics Research Letters*, Vol. 65, 7–79, 2017.
16. Lan, S.-W., M.-H. Weng, C.-Y. Hung, and S.-J. Chang, "Design of a compact ultra-wideband bandpass filter with an extremely broad stopband region," *IEEE Microwave and Wireless Components Letters*, Vol. 26, No. 6, 392–394, 2016.
17. Lan, S. W., M. H. Weng, C. Y. Hung, and S. J. Chang, "Design of a compact ultra-wideband bandpass filter with an extremely broad stopband region," *IEEE Microwave and Wireless Components Letters*, Vol. 26, No. 6, 392–394, 2016.
18. Zhang, R. and D. Peroulis, "Mixed lumped and distributed circuits in wideband bandpass filter application for spurious-response suppression," *IEEE Microwave and Wireless Components Letters*, Vol. 28, No. 11, 978–980, 2018.
19. Shi, S. Y., W. J. Feng, W. Q. Che, and Q. Xue, "Novel miniaturization method for wideband filter design with enhanced upper stopband," *IEEE Transactions on Microwave Theory And Techniques*, Vol. 61, No. 2, 817–826, 2013.
20. Shen, G. X., W. Q. Che, W. J. Feng, and Q. Xue, "Analytical design of compact dual-band filters using dual composite right-/left-handed resonators," *IEEE Transactions on Microwave Theory and Techniques*, Vol. 65, No. 3, 804–814, 2016.

21. Bo, Y., Z. Y. Lin, X. Cai, H. G. Hao, W. Luo, and W. Huang, "A novel compact crlh bandpass filter on CSRR-loaded substrate integrated waveguide cavity," *Progress In Electromagnetics Research M*, Vol. 75, 121–129, 2018.
22. Abdalla, M. A. and Z. Hu, "Composite right/left-handed coplanar waveguide ferrite forward coupled-line coupler," *IET Microwaves, Antennas & Propagation*, Vol. 9, No. 10, 1104–1111, 2015.
23. Abdalla, M. A. and Z. Hu, "Compact metamaterial coplanar waveguide ferrite tunable resonator," *IET Microwaves, Antennas and Propagation*, Vol. 10, No. 4, 406–412, 2016.
24. Wei, Z. H., J. Huang, Y. H. Geng, J. Li, and G. Q. Xu, "Compact broadband bandpass filter on quarter-mode substrate integrated waveguide loaded with CRLH interdigital slots," *Progress In Electromagnetics Research Letters*, Vol. 59, 85–91, 2016.
25. Ibrhim, A. A., M. A. Abdalla, and D. Budimir, "Coupled CRLH transmission lines for compact and high selective bandpass filters," *Microwave and Optical Technology Letters*, Vol. 59, No. 6, 1248–1251, 2017.
26. Mohan, M. P., A. Alphones, and M. F. Karim, "Triple band filter based on double periodic CRLH resonator," *IEEE Microwave and Wireless Components Letters*, Vol. 28, No. 3, 212–214, 2018.
27. Ibrahim, A. A., M. A. Abdalla, and W. A. E. Ali, "Small size and wide-band band pass filter with DGS/CRLH structures," *Applied Computational Electromagnetics Society Journal*, Vol. 34, No. 5, 777–783, 2019.
28. Choudhary, D. K., M. A. Abdalla, and R. K. Chaudhary, "Compact D-CRLH resonator for low pass filter with wide rejection band, high roll-off and transmission zeros," *Int. Journal of Microwave and Wireless Technologies*, Vol. 11, No. 5–6, 509–516, 2019.
29. Hassan, A. Y. and M. A. Abdalla, "A double optimized transmission zeros based on π-CRLH dual-band bandpass filter," *Progress In Electromagnetics Research Letters*, Vol. 84, 131–137, 2019.
30. Eleftheriades, G. V., "A generalized negative-refractive-index transmission-line (NRI-TL) metamaterial for dual-band and quad-band applications," *IEEE Microw. Wireless Compon. Lett.*, Vol. 17, No. 6, 415–417, 2007.
31. Rennings, A., S. Otto, J. Mosig, C. Caloz, and I. Wolff, "Extended composite right/left-handed (E-CRLH) metamaterial and its application as quadband quarter-wavelength transmission line," *Asia-Pacific Microwave Conference (APMC)*, 1405–1408, Japan, 2006.
32. Ahmed, K. U. and B. S. Vidree, "Fine control of filter performance based on composite right/left-handed metamaterial technology," *Int. J. of RF and Microwave Computer-Aided Engineering*, Vol. 24, 39–45, 2014.
33. Studniberg, M. and G. V. Eleftheriades, "A dual-band bandpass filter based on generalized negative-refractive-index transmission-lines," *IEEE Microw. & Wireless Comp. Lett.*, Vol. 19, 18–20, 2009.
34. Hagag, M. F. and M. A. Abdalla, "Ultra compact CPW dual band filter based on π-generalized metamaterial NRI transmission line," *Journal of Electromagnetic Waves and Applications*, Vol. 29, 1093–1103, 2015.
35. Fouad, M. A. and M. A. Abdalla, "A new π-T generalized metamaterial NRI transmission line for a compact CPW triple BPF applications," *IET Microw. Ant. & Propag.*, Vol. 2014, No. 8, 1097–1104, 2014.